

Comparative analysis of *p4ha1* and *p4ha2* expression during *Xenopus laevis* development

DAVIDE MARTINI^{1,#}, MARTINA GIANNACCINI^{1,#}, VIVIANA GUADAGNI^{1,#}, SILVIA MARRACCI¹, GUIDO GIUDETTI² and MASSIMILIANO ANDREAZZOLI^{*,1}

¹Unità di Biologia Cellulare e dello Sviluppo, Dipartimento di Biologia, Università di Pisa, Pisa, Italy and

²Istituto di Biorobotica, Scuola Superiore Sant'Anna, Pisa, Italy

ABSTRACT Collagen prolyl 4-hydroxylases (c-P4Hs) are evolutionary conserved enzymes whose activity is essential for the correct folding of stable triple helical molecules of collagen and collagen-like proteins. They play crucial roles in embryo development, connective tissue functional organization, tumor growth and metastasis. Despite the important function of these enzymes, little is known about their expression during vertebrate development. In this study, we determine and compare the previously undescribed spatio-temporal expression patterns of the *p4ha1* and *p4ha2* genes, which encode the main subunits containing the enzyme active site, during *Xenopus* development. The two genes are maternally inherited and share expression in dorsal mesoderm, branchial arches and their derivatives, as well as in the central nervous system, although with distinct spatio-temporal patterns. A major co-expression domain for *p4ha1* and *p4ha2* is represented by the developing notochord, where these genes are transcribed from early neurula stage to stage 42 tadpole, thus paralleling the profile of collagen II production and suggesting a coordination between collagen synthesis and its post-translational modifications.

KEY WORDS: *prolyl-hydroxylase, gene expression, development, Xenopus laevis, collagen*


Collagen prolyl 4-hydroxylases (c-P4Hs), located within the lumen of the endoplasmic reticulum (ER), are pivotal enzymes for the maturation of extracellular matrix proteins. They catalyze the 4-hydroxylation of the proline in -X-Pro-Gly- sequences of collagen and proteins with collagen-like sequences (Holster *et al.*, 2007). This reaction is essential for the correct folding of stable triple helical molecules of collagen, the most abundant protein in animals and the major component of connective tissue extracellular matrix (Shoulders and Raines, 2009). Accordingly, c-P4Hs catalyze the single most prevalent post-translational modification in animals and play a crucial role in embryo development, connective tissue functional organization, as well as tumor growth and metastasis (Holster *et al.*, 2007, Winter and Page, 2000). These enzymes are composed of dimers or tetramers of α and β subunits. The catalytic subunits are located in the α subunits while the β subunits are identical to the protein-disulfide isomerase (PDI) (Helaakoski *et al.*, 1989, Kivirikko *et al.*, 1990).

These enzymes are evolutionary conserved among animals from invertebrate to humans, as also shown by the ability of

heterodimers made by *D. melanogaster* or *C. elegans* α subunits and human PDI to catalyze collagen hydroxylation (Annunen *et al.*, 1999, Winter and Page, 2000).

In *C. elegans* two α subunits, namely *phy-1* and *phy-2*, as well as two β subunits, *pdi-1* and *pdi-2*, have been identified. In the nematode, the active enzyme is a $\alpha\beta$ dimer rather than a $\alpha_2\beta_2$ tetramer as in *D. melanogaster* and in vertebrates. *phy-1* and *phy-2* expression starts from midelongation stage and persist throughout adult stage. The highest expression of *phy-1* and *phy-2* is found in the hypodermal cells, which are also responsible for collagen synthesis and display a higher concentration of *phy-2*-positive cells. Consistently, the temporal expression pattern of *phy-1* and *phy-2* shows two peaks corresponding to that of cuticle collagen production (Winter and Page, 2000). In order to investigate the role of the *phy-1* and *phy-2* genes, Winter and colleagues performed RNA interference experiments demonstrating that impairment of

Abbreviations used in this paper: c-P4H, collagen prolyl 4-hydroxylase.

*Address correspondence to: Massimiliano Andreazzoli. Unità di Biologia Cellulare e dello Sviluppo, SS12 Abetone e Brennero, 4, I-56127 Pisa, Italy. Tel. +39-050-2211485; Fax: + 39-050-2211495. E-mail: massimiliano.andreazzoli@unipi.it -  <https://orcid.org/0000-0001-9633-204X>

#Note: The indicated authors contributed equally to this work.

Submitted: 24 April, 2019; Accepted: 15 May, 2019.

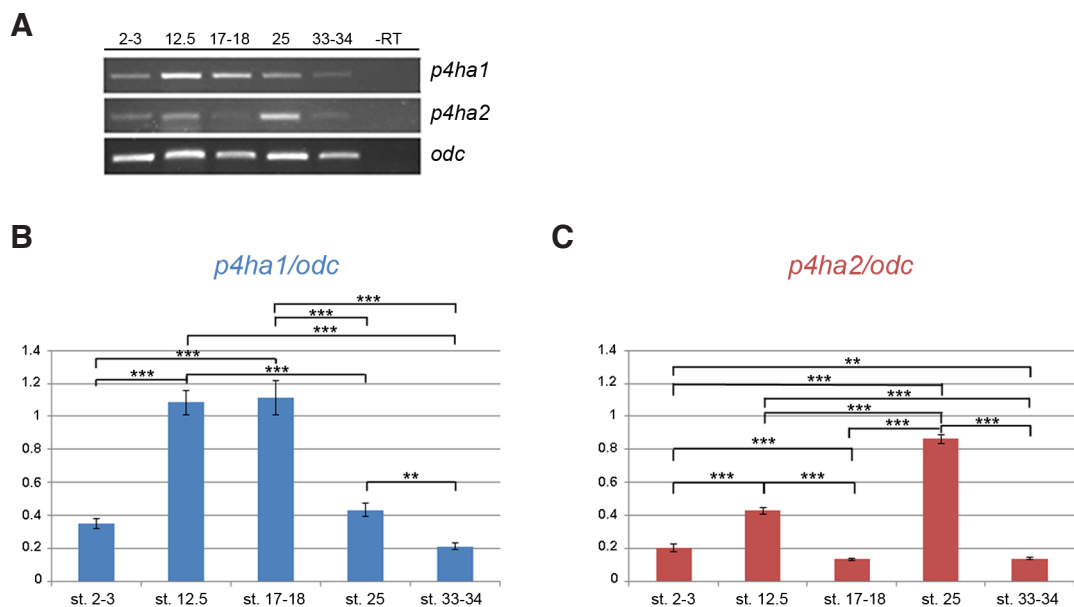


Fig. 1. RT-PCR analysis of *p4ha1* and *p4ha2* expression during *Xenopus* development. **(A)** *p4ha1* and *p4ha2* expression during embryonic development. cDNA derived from *Xenopus laevis* embryos at different stages (indicated at the top of the panel) was amplified using primers specific for *p4ha1*, *p4ha2* and ornithine decarboxylase gene (*odc*). For control reactions, reverse transcriptase was omitted (–RT). **(B,C)** Histogram representing the optical integrated density ratios between *p4ha1* **(B)**, *p4ha2* **(C)** and *odc* RT-PCR bands. (st.: stage). Significance: *p*-value < 0.05: *; *p*-value < 0.01: **; *p*-value < 0.001: ***.

phy-1 expression leads to a dumpy phenotype with shorter and fatter animals at larval L4 and adult stages. The dumpy phenotype is caused by abnormal cuticle deposition leading to improper exoskeleton morphology, probably due to collagen retention inside the cells as a consequence of the lack of prolyl hydroxylation. On the contrary, disruption of *phy-2* mRNA does not cause evident effects, possibly due to a partial redundancy of the enzymatic activity of the two subunits. However, the double knockdown of c-P4H α subunits displays more severe effects on *C. elegans* development leading to coiled larvae, dumpy adults and embryonic lethality in 89% of cases (Winter and Page, 2000).

In vertebrates, the α subunit is present in three isoforms: P4H α 1, P4H α 2, and P4H α 3. P4H α 1 represents the main form in most cell types, while the P4H α 2 is the prevalent one in chondrocytes, osteoblasts, endothelial and epithelial cells responsible for cartilage, cartilaginous bone and endothelium formation (Myllyharju, 2003). In humans, *P4HA1* is found to be highly expressed in fetal brain and liver. In the adult, the highest expression levels are observed in skeletal muscle, although *P4HA1* expression is detectable also in heart, placenta, liver and kidney as well as, at lower level, in the brain, lung and pancreas (Kukkola et al., 2003). The *P4HA2* gene is highly expressed in adult chondrocytes and endothelial cells. Lower levels of *P4HA2* were found in developing glomeruli of fetal kidney, according to histochemical analysis (Nissi et al., 2001). Interestingly, in the liver the bile ducts express the α 2 isoform while hepatocytes express at low level the α 1 isoform, indicating a different expression pattern and suggesting potential distinct roles for the two isoforms (Nissi et al., 2001). Indeed, it was shown that *P4HA1* is expressed preferentially by cells of mesenchymal origin and in developing tissues, whereas *P4HA2* is mainly expressed in differentiated cells (Nissi et al., 2001). Finally, the human *P4HA3* is expressed in both adult and fetal tissues but at a much lower level compared to the other two (Kukkola et al., 2003).

In vertebrates, the *in vivo* function was deeply investigated only for P4H α 1 in mouse knockout by Holster and colleagues in 2007. In contrast to heterozygotic mice, which appear to be normal, null embryos develop normally until stage E9, but soon after their

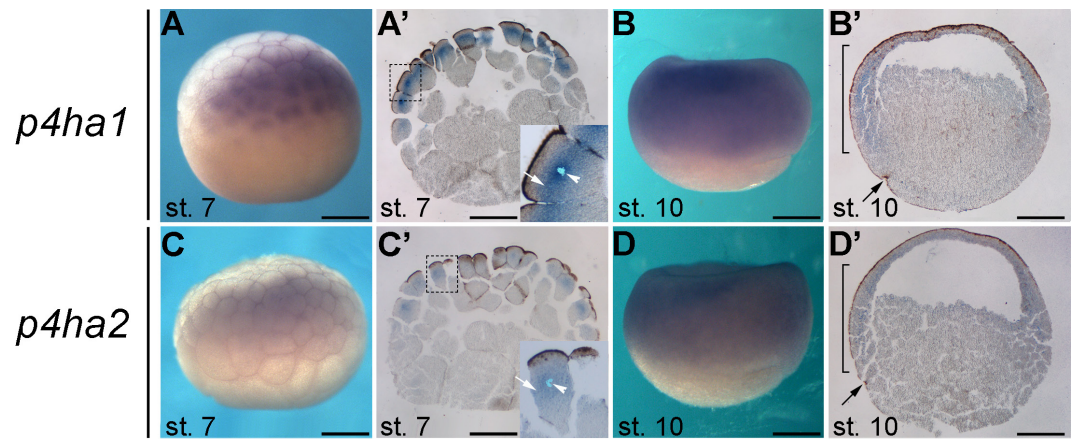
development begins to be retarded from stage E10.5 and they eventually die between stages E10.5–E11.5. In null embryos collagen IV is correctly synthesized but, without the prolyl hydroxylation by P4H α 1, is not properly assembled in functional triple helices, leading to the rupture of the basement membrane. Moreover, these collagen IV fibers have an increased diameter probably due to a reduced contact between the triple helices, which, together with their retention inside the cells, causes the dilatation of ER (Holster et al., 2007). As for *C. elegans*, developmental problems in mouse appear when collagen synthesis becomes crucial. Although the synthesis of collagen IV starts at blastula stage, the collected data indicate that the incorrect assembly of triple helices becomes incompatible with life only after stage E10.5, possibly because the mechanical pressure increases during development (Holster et al., 2007).

Accordingly, human mutations in *P4HA* genes are associated to specific genetic diseases. *P4HA1* mutations cause a disorder of connective tissue involving tendon, bone, muscle affecting also the eye (Zou et al., 2017) with the induction of high myopia. Similarly, mutations in *P4HA2* have been described as a cause for non-syndromic high myopia (Guo et al., 2015).

Moreover, several diseases are produced by c-P4Hs malfunctioning. For instance, inhibition of c-P4Hs by ascorbate deficiency causes scurvy (Smith and Talbot, 2010), while excessive levels of collagen production generates unwanted fibrotic response after cardiac infarction or wound healing (Fan et al., 2012 and references therein). Recently, an interesting role of c-P4Hs in tumor growth and metastasis has been demonstrated as well. It is known that collagen deposition and alignment enhance tumor cell proliferation and migration (Gilkes et al., 2013, Xiong et al., 2014). Accordingly, it was shown that hypoxia-inducible factor 1, a crucial factor for malignant cancer growth, induces enhanced invasion and metastasis also by increasing the expression of P4H α 1 and P4H α 2, (Gilkes et al., 2013). Moreover, the inhibition of P4H α 2 suppresses the aggressive phenotype and reduces cell proliferation in breast cancer (Xiong et al., 2014).

Because of the relevance of *Xenopus laevis* as a model system in embryo development and in biomedical research, in this study

Fig. 2. Whole mount *in situ* hybridization analysis of *p4ha1* and *p4ha2* during segmentation and gastrulation. Stages of embryos are indicated at the bottom left corner of each panel (st.: stage), while the analyzed gene is indicated to the left of each row. (A,C) Lateral view of stage 7 embryos; animal pole to the top, vegetal pole to the bottom. (A', C') Sagittal sections of the hybridized embryos shown in (A) and (C), respectively; the insets in (A',C'), indicated by the dashed line square in each panel, show the intracellular localization of the two transcripts in animal blastomeres; white arrowheads indicate Hoechst-stained nuclei, white arrows point to the cytoplasmic perinuclear expression. (B,D) Lateral view of stage 10 embryos; animal pole to the top, vegetal pole to the bottom. (B',D') Sagittal sections of the hybridized embryos shown in (B,D), respectively; black arrows point to the blastopore lip; brackets indicate the dorsal involuting mesoderm. Scale bars, 250 μ m.



we determine and compare the spatio-temporal expression pattern of *p4ha1* and *p4ha2*, encoding for the main subunits containing the peptide-substrate-binding domain and the enzyme active site, during *Xenopus* development.

Results and Discussion

Temporal expression

To analyze the temporal expression pattern of *p4ha1* and *p4ha2* during embryonic development, we performed RT-PCR assay on cDNAs obtained from *Xenopus* embryos at different developmental stages.

The two genes display both maternal and zygotic expression, being detected before and after the midblastula transition (stage 8, Fig. 1A). However, they show a quite different temporal expression profile. *p4ha1* expression is already detected at 2-3 cell stage and reaches the highest levels between early neurula (stages 12.5) and late neurula (stage 17-18), decreasing at later stages. (Fig. 1B). Differently, *p4ha2* displays a more dynamic expression during early development (Fig. 1C). It is expressed at 2-3 cell stage with an increase at stage 12.5, followed by a decrease at stages 17-

18 and reaching a maximum peak at stage 25. At stage 33-34, its expression declines again to the level observed at stages 17-18.

Spatial expression

The maternal transcripts of both genes are visible in the animal pole at blastula stage (stage 7) (Fig. 2 A,C) with a very similar pattern, although *p4ha2* displays lower expression levels at this stage. In particular, the intracellular localization of both transcripts is restricted to the perinuclear region (Fig. 2 A',C'). Also the zygotic expression at early gastrula stage (stage 10) is very similar for both genes (Fig. 2 B,D), diffusely expressed in the ectoderm and in the dorsal involuting mesoderm (Fig. 2 B',D', brackets).

At early neurula stage (stage 13), *p4ha1* and *p4ha2* are mainly expressed in the developing notochord, in line with the onset of collagen II production at stage 12.5 (Su *et al.*, 1991). Moreover, both genes show a weak expression in anterior regions of the neural plate, which extends dorsally in the case of *p4ha2* (Fig. 3 A,E). This pattern is maintained at stage 16 with *p4ha2* displaying a more diffuse expression in the anterior neural plate and in the cardiac progenitors' territory (Fig. 3F, red arrow)(Cizelsky *et al.*, 2013), excluding the cement gland primordium (Fig. 3 B,F ar-

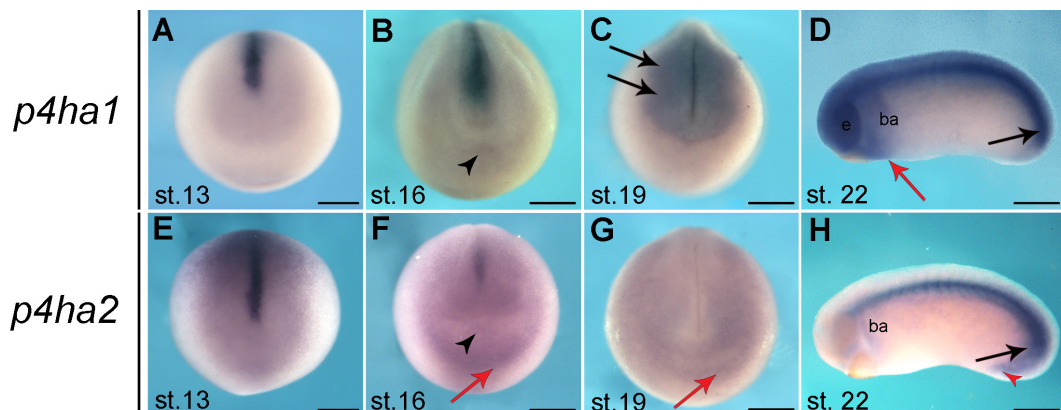


Fig. 3. Whole mount *in situ* hybridization analysis of *p4ha1* and *p4ha2* during neurulation. Stages of embryos are indicated at the bottom left corner of each panel (st.: stage), while the analyzed gene is indicated to the left of each row (A-C, E-G) Frontal view (dorsal to the top) of hybridized embryos at the indicated neurula stages. (D,H) Lateral view of hybridized stage 22 embryos; anterior is to the left. Black arrowhead in (B,F) indicate cement gland primordium; red arrows in (D,F,G) indicate cardiac progenitors. Black arrows in (C) indicate the neural crests. Black arrows in (D,H) indicate the posterior wall and the red arrowhead in (H) the proctodeum. Abbreviations: ba, branchial arches; e, eye. Scale bars, 250 μ m.

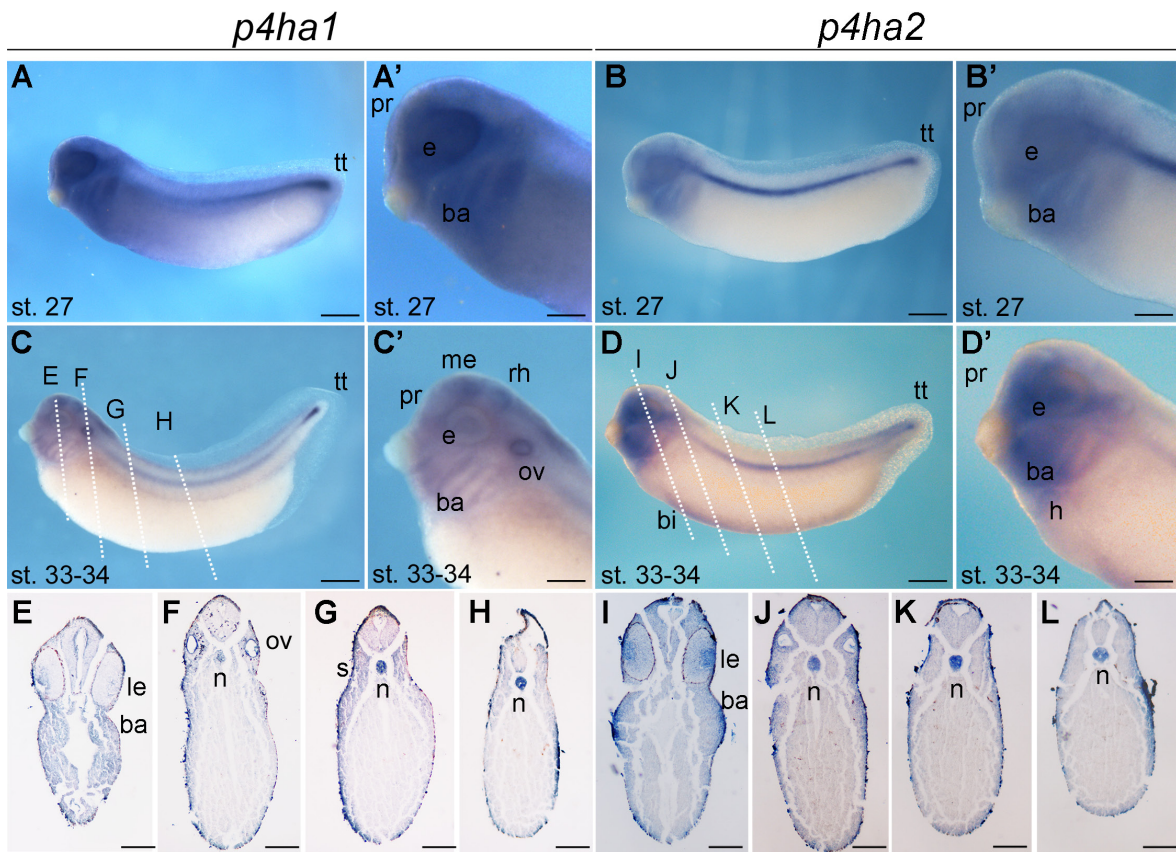


Fig. 4. Whole mount *in situ* hybridization analysis of *p4ha1* and *p4ha2* in tadpole embryos. Embryo stages (st.) are indicated at the bottom left corner of each panel, while the analyzed gene is indicated at the top. (A', B', C', D') magnified views of (A, B, C, D), respectively. In panels (A-D') anterior is to the left. Dashed lines in (C) point to the planes of the sections shown in (E-H). Dashed lines in (D) indicate the planes of the sections shown in (I-L). Abbreviations: ba, branchial arches; bi, blood islands; e, eye; h, heart; le, lens; me, mesencephalon; n, notochord; ov, otic vesicle; pr, prosencephalon; rh, rhombencephalon, s, somites; tt, tail tip. Scale bars in (A, B, C, D), 500 μ m; in (A', B', C', D'), 250 μ m; in (E-H, I-L), 200 μ m.

rowhead). At late neurula stage (stage 19), *p4ha1* expression is clearly activated in anterior central nervous system (Fig. 3C) and the migrating neural crest cells (Fig. 3C, black arrows). At the same stages, *p4ha2* expression appears to be remarkably low, detectable as a diffuse *in situ* hybridization signal in the anterior neural plate and in the cardiac progenitors' territory (Fig. 3G, red arrow). At early tailbud stage (stage 22), both genes are highly expressed in the notochord (Fig. 3D, H) and in the tail bud, which is composed by the chordoneural hinge and the posterior wall (Fig. 3D, H black arrows), with *p4ha2* extending in the proctodeum (Fig. 3H, red arrowhead) (Beck and Slack, 1998). Furthermore, *p4ha1* is expressed in the central nervous system, including the eyes, in neural crest cells migrated into the branchial arches, which in part express also *p4ha2* (Fig. 3D, H), and, posteriorly to the cement gland, in the presumptive cardiac progenitors' territory (Fig. 3D, red arrow). As development proceeds, the predominant notochord expression is maintained for both transcripts, accordingly with collagen gene expression and protein synthesis (Su *et al.*, 1991).

At stage 27, *p4ha1* is expressed in the eye, more intensively in its dorsal peripheral region, branchial arches and faintly in somites and proctodeum (Fig. 4A, A'). At this stage the notochord expression of *p4ha1* displays a gradient decreasing from the posterior to the anterior end (Fig. 4A), whereas *p4ha2* is highly expressed in the entire notochord (Fig. 4B). Compared to *p4ha1* (Fig. 4A'),

p4ha2 shows a lower expression level in the head and in the neural crest streams (Fig. 4B').

At stage 33/34 the expression profile of the two genes displays many similarities, but also some differences. Both genes are expressed in different regions of nervous system, lens, branchial arches, notochord and in the tip of the growing tail (Fig. 4C, C', D, D'). However, hybridization signal of *p4ha1* marks also the otic vesicle and, to a lower extent, the dorsal and ventral borders of the somitic mesoderm (Fig. 4C', F, G). Differently, *p4ha2* is expressed in the heart, the blood islands and the dorsal somitic mesoderm of the caudal region (Fig. 4D, D'). Histological sections of hybridized embryos show a weak *p4ha1* signal in the central nervous system, while *p4ha2* displays a more specifically localized expression in the prosencephalon (Fig. 4E-L). Moreover, *p4ha1* expression signal is visible in branchial arches, otic vesicles, notochord and weakly in somites (Fig. 4E-H), while *p4ha2* is mainly detected in lens, branchial arches, and notochord (Fig. 4I-L).

Finally, we compared the expression profile of *p4ha1* and *p4ha2* in stage 42 embryos. In the head, *p4ha1* is expressed in a region corresponding to the presumptive Meckel's cartilage, in discrete sites located dorso-laterally with respect to the pharynx (arrows in Fig. 5A) and in otic vesicles (Fig. 5B), while *p4ha2* hybridization signal is present in infraorbital cartilage and cranial muscles, as well as in the mesencephalon, rhombencephalon and otic

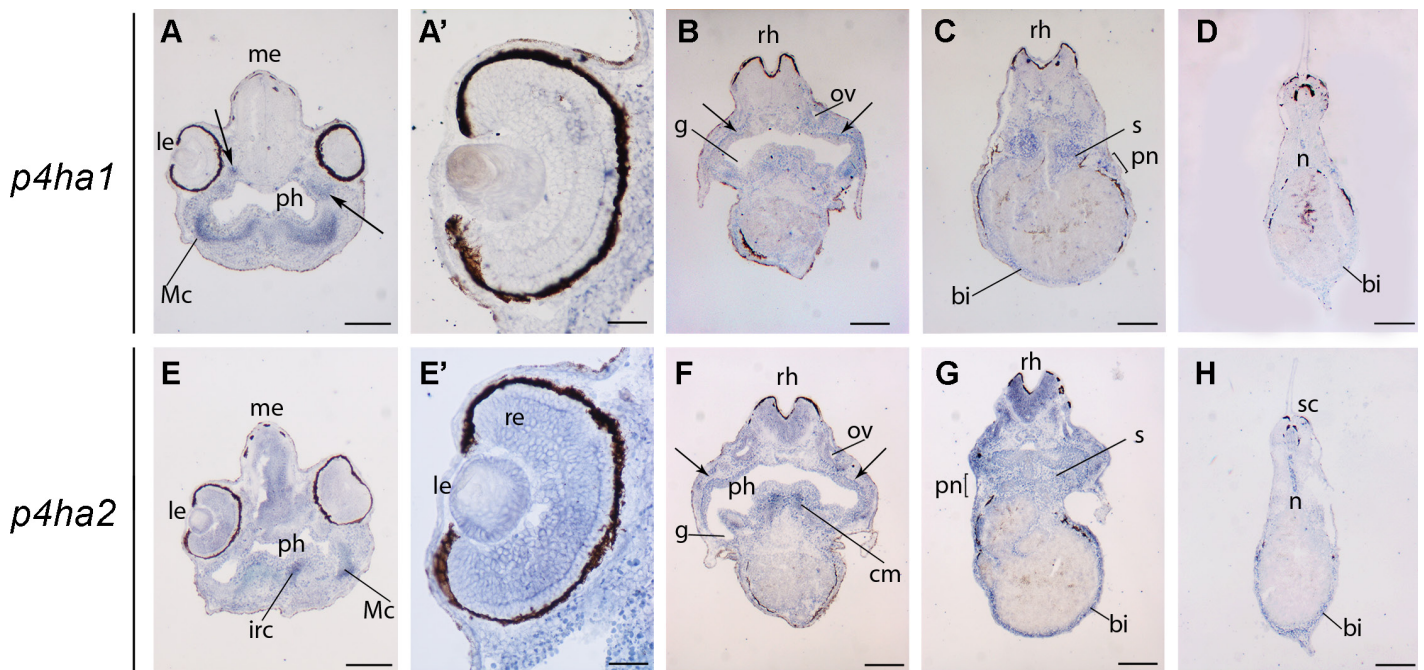


Fig. 5. Cryosections of stage 42 embryos hybridized with *p4ha1* (A-D) and *p4ha2* (E-H) probes. Black arrows in (A) indicate regions located dorso-laterally with respect to the pharynx, labeled with *p4ha1*. Black arrows in (B,F) point to regions surrounding the internal gills, labeled with *p4ha1* and *p4ha2*. Abbreviations: Bi, blood islands; cm, cranial muscles; g, gill chamber; irc, infrastratal cartilage; le, lens; Mc, presumptive Meckel's cartilage; me, mesencephalon; n, notochord; ov, otic vesicle; ph, pharynx; pn, pronephros; re, retina; rh, rhombencephalon; s, somites; sc, spinal cord. Scale bars in (A,B,C,D,E,F,G,H) 200 μ m; in (A', E') 50 μ m.

vesicles (Fig. 5E-G). Both genes also display specific expression in regions that bilaterally surround the internal gills (arrows in Fig. 5B, F). Moreover, *p4ha2*, but not *p4ha1*, is expressed also in the eye (Fig. 5A', 5E'), where it is detected in the retina and, consistently with immunolocalization of prolyl 4-hydroxylase in rabbit, in the lens (Saika *et al.*, 1998).

In the trunk-tail regions, expression of *p4ha2* and *p4ha1* is detected in somites, pronephros and blood islands, although at different expression levels. In particular, *p4ha2* is also expressed in the spinal cord. Notably, at this stage both genes are not expressed in the notochord, except for the most terminal region (Fig. 5 D,H), coherently with the decrease of collagen gene expression at similar stages in *Xenopus laevis* embryos (Su *et al.*, 1991).

In conclusion, we found that the mRNA expression of both subunits of the α prolyl hydroxylase is spatially and temporally regulated during *Xenopus* embryogenesis, showing many sites of co-expression in embryos at different developmental stages, especially in the notochord and in neural crest-derived regions. However, each of the two genes also displays some unique expression sites suggesting that they are also differentially regulated and may potentially play specific roles during development. In particular, *p4ha2* displays a specific expression in early heart territory, as well as in blood islands and in the lens, allowing to speculate a putative function in differentiation of these structures. Remarkably, we observed that the expression of both genes coherently correlate with the presence of collagen in the notochord during *Xenopus* development, indicating the existence of a coordination between tropocollagen synthesis and its post-translational modifications to generate mature fibrillary collagen (Gorres and Raines, 2010)

Materials and Methods

RNA extraction and RT-PCR analysis

Total RNA was extracted from embryos using Mini RNA Isolation Kit (Nucleospin RNA XS, Macherey Nagel). First strand cDNA was synthesized using Superscript II Reverse Transcriptase (Invitrogen), from 1 μ g of total RNA. RT-PCR analysis was performed using the following gene-specific sets of primers:

p4ha1-forward: 5'-TCATTTCCCCGCAAATACA-3'
p4ha1-reverse: 5'-TTCCCTTGACCTTTCAATG-3'
p4ha2-forward: 5'-ACGAGCTGGAAGCAATCTGA-3'
p4ha2-reverse: 5'-TTGACTCCCTCTCCTCGACA-3'
odc-forward: 5'-GGGCTGGATCGTATCGTAGA-3'
odc-reverse: 5'-CTTCAGGGAGAATGCCATGT-3'

Ornithine decarboxylase (*odc*) was used as housekeeping gene for normalization. The optical density was calculated using the ImageJ software. Data are expressed as mean \pm standard deviation; n=9 samples for each embryonic stage in three independent experiments. Statistical analysis was carried out using ANOVA followed by post-hoc Tukey's Multiple range test. p-values <0.05 were considered to be statistically significant.

In situ hybridization

Xenopus embryos were generated and staged as previously described (Marracci *et al.*, 2015). Whole-mount *in situ* hybridization was performed as previously described (Watanabe *et al.*, 2002). Probes for *p4ha1* was transcribed from cDNA clone XL014a11 (GenBank Acc. n. BJ046645) and *p4ha2* from cDNA clone XL094g09 (GenBank Acc. n. BJ071438).

Antisense transcripts were obtained by plasmid linearization with EcoRI and *in vitro* transcription using T7 RNA polymerase (Roche). Sense transcripts were used as negative control (data not shown). *in situ* hybridization on cryostat sections (12 μ m thick), as well as sections (15 μ m thick) of paraffin-embedded embryos were performed as previously

described (D'Autilia et al., 2010, Marracci et al., 2015).

Acknowledgments

The authors are grateful to Naoto Ueno, for generously providing the plasmids (XL014a11 and XL094g09) and thank Marzia Fabbri, Donatella De Matienzo and Elena Landi for technical assistance, and Salvatore Di Maria for frog care.

References

- ANNUNEN, P., KOIVUNEN, P. and KIVIRIKKO, K.I. (1999). Cloning of the alpha subunit of prolyl 4-hydroxylase from *Drosophila* and expression and characterization of the corresponding enzyme tetramer with some unique properties. *J Biol Chem* 274: 6790-6796.
- BECK, C.W. and SLACK, J.M. (1998). Analysis of the developing *Xenopus* tail bud reveals separate phases of gene expression during determination and outgrowth. *Mech Dev* 72: 41-52.
- CIZELSKY, W., HEMPEL, A., METZIG, M., TAO, S., HOLLEMANN, T., KUHL, M. and KUHL, S.J. (2013). *sox4* and *sox11* function during *Xenopus laevis* eye development. *PLoS One* 8: e69372.
- D'AUTILIA, S., BROCCOLI, V., BARSACCHI, G. and ANDREAZZOLI, M. (2010). *Xenopus* Bsx links daily cell cycle rhythms and pineal photoreceptor fate. *Proc Natl Acad Sci USA* 107: 6352-6357.
- FAN, D., TAKAWALE, A., LEE, J. and KASSIRI, Z. (2012). Cardiac fibroblasts, fibrosis and extracellular matrix remodeling in heart disease. *Fibrogen. Tissue Rep.* 5: 15.
- GILKES, D.M., BAJPAI, S., CHATURVEDI, P., WIRTZ, D. and SEMENZA, G.L. (2013). Hypoxia-inducible factor 1 (HIF-1) promotes extracellular matrix remodeling under hypoxic conditions by inducing P4HA1, P4HA2, and PLOD2 expression in fibroblasts. *J Biol Chem* 288: 10819-10829.
- GORRES, K.L. and RAINES, R.T. (2010). Prolyl 4-hydroxylase. *Crit Rev Biochem-MolBiol* 45: 106-124.
- GUO, H., TONG, P., LIU, Y., XIA, L., WANG, T., TIAN, Q., LI, Y., HU, Y., ZHENG, Y., JIN, X. et al., (2015). Mutations of P4HA2 encoding prolyl 4-hydroxylase 2 are associated with nonsyndromic high myopia. *Genet Med* 17: 300-306.
- HELAAKOSKI, T., VUORI, K., MYLLYLÄ, R., KIVIRIKKO, K.I. and PIHLAJANIEMI, T. (1989). Molecular cloning of the alpha-subunit of human prolyl 4-hydroxylase: the complete cDNA-derived amino acid sequence and evidence for alternative splicing of RNA transcripts. *Proc Natl Acad Sci USA* 86: 4392-4396.
- HOLSTER, T., PAKKANEN, O., SOININEN, R., SORMUNEN, R., NOKELAINEN, M., KIVIRIKKO, K.I. and MYLLYHARJU, J. (2007). Loss of assembly of the main basement membrane collagen, type IV, but not fibril-forming collagens and embryonic death in collagen prolyl 4-hydroxylase I null mice. *J Biol Chem* 282: 2512-2519.
- KIVIRIKKO, K.I., HELAAKOSKI, T., TASANEN, K., VUORI, K., MYLLYLÄ, R., PARKKONEN, T. and PIHLAJANIEMI, T. (1990). Molecular biology of prolyl 4-hydroxylase. *Ann N Y Acad Sci* 580: 132-142.
- KUKKOLA, L., HIETA, R., KIVIRIKKO, K.I. and MYLLYHARJU, J. (2003). Identification and characterization of a third human, rat, and mouse collagen prolyl 4-hydroxylase isoenzyme. *J Biol Chem* 278: 47685-47693.
- MARRACCI, S., MARTINI, D., GIANNACCINI, M., GIUDETTI, G., DENTE, L. and ANDREAZZOLI, M. (2015). Comparative expression analysis of *pfnd6a* and *tcp1alpha* during *Xenopus* development. *Int J Dev Biol* 59: 235-240.
- MYLLYHARJU, J. (2003). Prolyl 4-hydroxylases, the key enzymes of collagen biosynthesis. *Matrix Biol* 22: 15-24.
- NISSI, R., AUTIO-HARMAINEN, H., MARTTILA, P., SORMUNEN, R. and KIVIRIKKO, K.I. (2001). Prolyl 4-hydroxylase isoenzymes I and II have different expression patterns in several human tissues. *J Histochem Cytochem* 49: 1143-1153.
- SAIKA, S., KAWASHIMA, Y., MIYAMOTO, T., TANAKA, S., OKADA, Y., YAMANAKA, O., KATOH, T., OHNISHI, Y., OHMI, S., OOSHIMA, A. et al., (1998). Immunolocalization of prolyl 4-hydroxylase in rabbit lens epithelial cells. *J Cataract Refract Surg* 24: 1261-5.
- SHOULDERS, M.D. and RAINES, R.T. (2009). Collagen structure and stability. *Annu Rev Biochem* 78: 929-958.
- SMITH, T.G. and TALBOT, N.P. (2010). Prolyl hydroxylases and therapeutics. *Antioxid Redox Signal* 12: 431-433.
- SU, M.W., SUZUKI, H.R., BIEKER, J.J., SOLURSH, M. and RAMIREZ, F. (1991). Expression of two nonallelic type II procollagen genes during *Xenopus laevis* embryogenesis is characterized by stage-specific production of alternatively spliced transcripts. *J Cell Biol* 115: 565-575.
- WATANABE, M., REBBERT, M.L., ANDREAZZOLI, M., TAKAHASHI, N., TOYAMA, R., ZIMMERMAN, S., WHITMAN, M., DAWID, I.B. (2002). Regulation of the Lim-1 gene is mediated through conserved FAST-1/FoxH1 sites in the first intron. *Dev Dyn* 225: 448-456.
- WINTER, A.D. and PAGE, A.P. (2000). Prolyl 4-hydroxylase is an essential procollagen-modifying enzyme required for exoskeleton formation and the maintenance of body shape in the nematode *Caenorhabditis elegans*. *Mol Cell Biol* 20: 4084-4093.
- XIONG, G., DENG, L., ZHU, J., RYCHAHOU, P.G. and XU, R. (2014). Prolyl-4-hydroxylase alpha subunit 2 promotes breast cancer progression and metastasis by regulating collagen deposition. *BMC Cancer* 14: 1.
- ZOU, Y., DONKERVOORT, S., SALO, A.M., FOLEY, A.R., BARNES, A.M., HU, Y., MAKAREEVA, E., LEACH, M.E., MOHASSEL, P., DASTGIR, J. et al., (2017). P4HA1 mutations cause a unique congenital disorder of connective tissue involving tendon, bone, muscle and the eye. *Hum Mol Genet* 26: 2207-2217.

Further Related Reading, published previously in the *Int. J. Dev. Biol.*

Modeling and quantification of cancer cell invasion through collagen type I matrices

Olivier De Wever, An Hendrix, Astrid De Boeck, Wendy Westbroek, Geert Braems, Shahin Emami, Michèle Sabbah, Christian Gespach and Marc Bracke

Int. J. Dev. Biol. (2010) 54: 887-896
<https://doi.org/10.1387/ijdb.092948ow>

Skin development in bony fish with particular emphasis on collagen deposition in the dermis of the zebrafish (*Danio rerio*)

Dominique Le Guellec, Ghislaine Morvan-Dubois and Jean-Yves Sire

Int. J. Dev. Biol. (2004) 48: 217-231
<http://www.intjdevbiol.com/web/paper/15272388>

Role of the extracellular matrix and growth factors in skull morphogenesis and in the pathogenesis of craniosynostosis

P Carinci, E Becchetti and M Bodo

Int. J. Dev. Biol. (2000) 44: 715-723
<http://www.intjdevbiol.com/web/paper/11061436>

Endochondral bone formation in toothless (osteopetrotic) rats: failures of chondrocyte patterning and type X collagen expression

S C Marks, C Lundmark, C Christersson, T Wurtz, P R Odgren, M F Seifert, C A Mackay, A Mason-Savas and S N Popoff

Int. J. Dev. Biol. (2000) 44: 309-316
<http://www.intjdevbiol.com/web/paper/10853827>

Establishing laminin, collagen IV and chondroitin sulfate patterns in otocystogenesis

S Callejo, M Barbosa, J A Moro, A Gato, M I Alonso and E Barbosa

Int. J. Dev. Biol. (1996) 40: S249-S250
<http://www.intjdevbiol.com/web/paper/9087783>

Differences in collagen and cell density during normal and dexamethasone-treated secondary palate development in two strains of mice

M A Montenegro, M Rojas, S Dominguez and J Posada

Int. J. Dev. Biol. (1996) 40: S245-S246
<http://www.intjdevbiol.com/web/paper/9087781>

Effects of "in situ" vitamin E on fibroblast differentiation and on collagen fibril development in the regenerating tendon

R González Santander, M A Plasencia Arriba, G Martínez Cuadrado, M González-Santander Martínez and M Monteagudo de la Rosa

Int. J. Dev. Biol. (1996) 40: S181-S182
<http://www.intjdevbiol.com/web/paper/9087752>

